Dyes and Pigments 96 (2013) 63–70

Contents lists available at SciVerse ScienceDirect

Dyes and Pigments

journal homepage: www.elsevier.com/locate/dyepig

5-Phenyl-1,2,3,4-tetrahydronaphthalene derivatives: Synthesis, spectroscopic and electrochemical investigation

Marek Pietrzak*, Agnieszka Bajorek

University of Technology and Life Sciences, Faculty of Chemical Technology and Engineering, Seminaryjna 3, 85-326 Bydgoszcz, Poland

ARTICLE INFO

Article history:
Received 21 May 2012
Received in revised form
12 July 2012
Accepted 13 July 2012
Available online 20 July 2012

Keywords:
Biphenyls
Synthesis
Spectroscopic and electrochemical properties
Red-edge effect
Fluorescence probes

ABSTRACT

A series of novel dyes, whose structures are based on 5-phenyl-1,2,3,4-tetrahydronaphthalene skeleton have been fully synthesized and characterized. The dyes were prepared in two-stage synthesis reaction. The 2-cyano-3-[4-aminophenyl]-2-propenamide derivatives, and the final dyes were characterized by ^{1}H and ^{13}C NMR spectroscopy and their purity was checked by thin-layer chromatography and finally HPLC. The spectroscopic properties of the prepared dyes were studied in four different solvents.

© 2012 Elsevier Ltd. All rights reserved.

1. Introduction

In recent years dyes have been widely used as fluorescence probes. They are spectroscopic tools used in chemistry, biology and physics for monitoring specific properties of the medium in which they are incorporated. It is possible because their fluorescence is sensitive to changes in temperature, polarity, viscosity, pH or rigidity of the environment [1–4]. Readers can find many articles which focus on studies based on the concept of the changing of fluorescence depolarization, fluorescence yield, the position of fluorescence maxima [5,6] and others for the monitoring of the properties of environment [7,8]. In recent years, spectroscopic probes have been extensively used in the detection of nucleic acids and the determination of their structure [9,10]. The fluorimetric probes which show significant red-edge effect are found to be one of important type of probes [11–13]. Described in our earlier papers derivatives of ethyl 5-(4-aminophenyl)-3-amino-2,4-dicyanobenzoate are examples of such probes [14,15]. Studying the solvent polarity effect on the spectroscopic properties of the compounds, it was found that conformations with coplanar donor and acceptor groups absorb and emit at longer wavelengths than those observed for donor–acceptor groups oriented orthogonally. Equilibrium between these two forms is controlled by solvent properties and, due to the low energy of the barrier separating these forms, can be, in part, controlled by viscosity and the temperature of environment.

In the present paper we report on the synthesis of new organic molecules and the characterization of their photophysical and electrochemical properties. The tested compounds possess strong electron acceptors substituents in the first phenyl ring and a strong electron donor group in the *para* or *meta* position in the second ring. Compounds of similar structure have previously been synthesized by several different methods [16–20]. In this study, the synthesis of the dyes was implemented using a modification of the method described earlier by Elgemeie and co-workers [20] giving the possibility of obtaining compounds with different amino groups.

2. Experimental

2.1. Measurements

All starting reagents and solvents (reagent grade) were purchased from Aldrich Chemical Co. and Lancaster Chemical Co. and were used without further purification.

Melting points (uncorrected) were determined on the Boëthius apparatus.

2.1.1. Spectral measurements

The ^{1}H (200 MHz) and ^{13}C (50 MHz) NMR spectra were recorded with the use of a Varian spectrometer Gemini 200. Dimethylsulfoxide

* Corresponding author. Tel.: +48 52 374 9034; fax: +48 52 374 9009.
E-mail address: marek@utp.edu.pl (M. Pietrzak).

0143-7208/$ – see front matter © 2012 Elsevier Ltd. All rights reserved.
http://dx.doi.org/10.1016/j.dyepig.2012.07.009

(DMSO-d_6) was used as the solvent and tetramethylsilane as the internal standard.

The IR spectra of the synthesized compounds were recorded using a Bruker spectrophotometer Vector 22, in the range 400–4500 cm^{-1}, by KBr pellet technique.

The UV–vis absorption spectra were recorded using a Shimadzu UV–vis Multispec-1501 spectrophotometer, and fluorescence spectra were obtained with a Hitachi F-4500 spectrofluorimeter. The fluorescence quantum yields for the dyes in the tested solvents were determined as follows. The fluorescence spectrum of a dilute ($A = 0.1$) dye solution was recorded by excitation at the absorption band maximum of the reference. A dilute Coumarin I in ethanol solution ($\Phi = 0.64$ [21]) was used as a reference. The fluorescence spectrum of Coumarin I was obtained by excitation at its absorption peak at 366 nm. The fluorescence quantum yield of the tested dyes (Φ_{dye}) was calculated using equation:

$$\Phi_{dye} = \Phi_{ref} \frac{I_{dye} A_{ref}}{I_{ref} A_{dye}} \cdot \frac{n_{dye}^2}{n_{ref}^2}$$

where Φ_{ref} is the fluorescence quantum yield of the reference (Coumarin I) sample in ethanol, A_{dye} and A_{ref} are the absorbances of the dye and reference samples at the excitation wavelengths (366 nm), I_{dye} and I_{ref} are the areas (in arbitrary units) under the corrected fluorescence spectra for the dyes and reference samples, n_{dye} and n_{ref} are the refractive indices of the solvents used for the dyes and the reference, respectively.

2.1.2. Electrochemical measurements

The oxidation potentials of the dyes were measured by cyclic voltammetry using an Electroanalytical Cypress System Model CS-1090. The typical three-electrode setup was employed for electrochemical measurements. The electrolyte was 0.1 M tetrabutylammonium perchlorate in dry acetonitrile, which was purged with argon prior to a measurement. Platinum 1 mm electrode was applied as working electrode and platinum and Ag/AgCl were used as auxiliary and reference electrodes, respectively.

2.1.3. High performance liquid chromatography

A Waters 1525 Binary HPLC Pump coupled to a Waters 2489 UV/visible detector and a Symmetry C18 column (3.5 μm, 4.6 × 75 mm) was used.

DFT calculations were carried out using B3LYP/6-311G(2d,p) method to estimate the ground state dipole moments of the dye molecules under investigation. All calculations were carried out with Gaussian 03 program [22].

2.2. Synthesis

2.2.1. Aldehydes

4-(Dimethylamino)benzaldehyde (**1b**) and 4-(diethylamino) benzaldehyde (**1c**) were purchased from Aldrich. The synthesis of 4-(dimethylamino)-2,3-dimethylbenzaldehyde (**1g**) and 4-(dimethylamino)-2,5-dimethylbenzaldehyde (**1h**) are described elsewhere [23], other aldehydes were synthesized according to the procedures found in literature [24,25].

A general method for the synthesis of the 2-cyano-3-[4-aminophenyl]-2-propenamide derivatives (**2a**–**n**) is presented in Scheme 1 (general procedure (A)). These compounds were obtained using *p*-aminobenzaldehydes and cyanoacetamide, adopting the method described in literature [26].

2.2.2. General procedure (A)

To a solution of appropriate *p*-aminobenzaldehyde **1a**–**n** (20 mmol) and cyanoacetamide (20 mmol) in ethanol (20 ml) a few drops of potassium hydroxide solution (10% in water) at 50 °C was added. The solution was set aside for seven hours at room temperature. The precipitate was filtered off and recrystallized from ethanol.

Characteristics of the synthesized propenamides are presented in Table 1.

The procedure described by Elgemeie and co-workers, was adapted to the synthesis of tested dyes, 3,4′-diamino-2,4-dicyanobiphenyl derivatives [20]. The dyes were prepared according to the method presented in Scheme 2 (general procedure (B)).

2.2.3. General procedure (B)

To a magnetically stirred solution of appropriate amide **2a**–**n** (10 mmol) and cyclohexylidenepropanedinitrile (10 mmol) in anhydrous ethanol (50 ml), piperidine (1 ml) was added. The mixture was then heated under reflux for 6 h. The solution was cooled and filtered. The residue was recrystallized from ethanol.

2.2.4. Compound *3o*

Compound **3o** was obtained by reducing the corresponding nitro compound, as shown in Scheme 3. Reagents: (i) cyanoacetamide, ethanol, KOH_{aq}, 50 °C to room temperature (according to general procedure (A)); (ii) cyclohexylidenepropanedinitrile, anhydrous ethanol, piperidine, reflux (according to general procedure (B)); (iii) tin powder, hydrochloric acid, ethanol.

3. Results and discussion

3.1. Synthesis of dyes

Thirteen dyes have been synthesized in a two-stage reaction. In the first stage, the appropriate 2-cyano-3-[4-aminophenyl]-2-propenamides were obtained from *p*-aminobenzaldehyde and cyanoacetamide, (Scheme 1, compounds **2a**–**n**). The structural analysis of the compounds is presented in Table 1 and Supplementary data. In the second stage, the 2-cyano-3-[4-aminophenyl]-2-propenamides reacted with cyclohexylidenepropanedinitrile (Scheme 2, compounds **3a**–**n**) yielding corresponding dyes. The reaction was carried out in anhydrous ethanol using piperidine as a catalyst. The

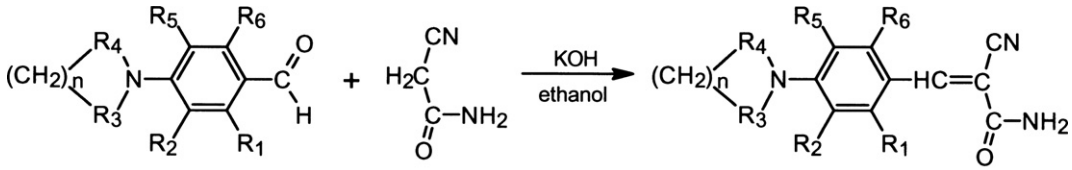

1a-n **2a-n**

where: R_1, R_6 : H, CH_3, R_2, R_5 : H, CH_3, $-CH_2-$ R_3, R_4 : H, CH_3, C_2H_5, $-CH_2-$ n : 2, 3

Scheme 1. A general route for the synthesis of 2-cyano-3-[4-aminophenyl]-2-propenamide derivatives.

Table 1
Structures, characteristics and basis spectroscopic properties of 2-cyano-3-[4-aminophenyl]-2-propenamide derivatives.

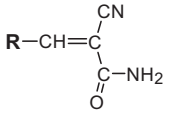

Ab.	**R-**	λ_{max}^{abs} [nm][a] (ε_{max}) [M^{-1} cm^{-1}]	Yield %	Melting point [°C], ^1H and ^{13}C NMR (DMSO-d_6) δ [ppm], IR (KBr) ν [cm^{-1}]
2a	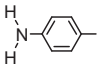	392 (38900)	75	M.p.: decomp. 235–240; ^1H NMR: 7.87 (s, 1H, –CH═), 7.70 (d, J = 8.8 Hz, 2H), 7.48 (br, s, 2H, C(O)NH_2), 6.62 (d, J = 8.8 Hz, 2H), 6.38 (s, 2H, ArNH_2); ^{13}C NMR: 163.9 (CO), 153.7 (C), 150.6 (CH), 133.1 (CH), 118.6 (C), 118.2 (C), 113.4 (CH), 96.3; IR (KBr): 2203 (C≡N), 1698 (C═O), 1643, 1613, 1515, 1346, 1180, 828
2b	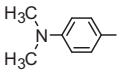	412 (43200)	82	M.p.: 197–198; ^1H NMR: 7.95 (s, 1H, –CH═), 7.84 (d, J = 8.8 Hz, 2H), 7.50 (br, s, 2H, NH_2), 6.80 (d, J = 9 Hz, 2H), 3.04 (s, 6H, $N(CH_3)_2$); IR (KBr): 2201 (C≡N), 1680 (C═O), 1611 (C═C), 1525, 1368, 1191, 810
2c	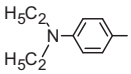	419 (44800)	66	M.p.: 135–136; ^1H NMR: 7.92 (s, 1H, –CH═), 7.82 (d, J = 9.2 Hz, 2H), 7.46 (br, s, 2H, NH_2), 6.78 (d, J = 9.2 Hz, 2H), 3.43 (q, J = 6.8 Hz, 4H, NCH_2), 1.11 (t, J = 7 Hz, 6H, CH_3); ^{13}C NMR: 163.9 (CO), 150.6 (C), 150.2 (CH), 132.9 (CH), 118.3 (C), 118.0 (C), 111.1 (CH), 96.4 (C), 43.9 (NCH_2), 12.4 (CH_3); IR (KBr): 2207 (C≡N), 1690 (C═O), 1666, 1611 (C═C), 1518, 1354, 1188, 825
2d	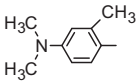	422 (37100)	83	M.p.: 222–224; ^1H NMR: 8.16 (s, 1H, –CH═), 8.10 (d, J = 9 Hz, 1H), 7.54 (br, s, 2H, NH_2), 6.71–6.62 (m, 3H), 3.02 (s, 6H, $N(CH_3)_2$), 2.36 (s, 3H, ArCH_3); IR (KBr): 2201 (C≡N), 1697 (C═O), 1616 (C═C), 1557, 1367, 1109, 790
2e	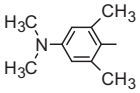	407 (15500)	83	M.p.: decomp. 185; ^1H NMR: 8.23 (s, 1H, –CH═), 7.87 oraz 7.68 (s, 2H, NH_2), 6.49 (s, 2H), 2.94 (s, 6H, $N(CH_3)_2$), 2.23 (s, 6H, ArCH_3); ^{13}C NMR: 163.1 (CO), 152.2, 150.7, 137.4, 119.7, 116.5, 111.3, 110.8, 39.7 ($N(CH_3)_2$), 20.7 (ArCH_3); IR (KBr): 2217 (CN), 1691 (C═O), 1574, 1368, 1150, 809
2f	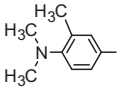	385 (19500)	39	M.p.: 118–120; ^1H NMR: 8.01 (s, 1H, –CH═), 7.78–7.72 (m, 3H), 7.61 (br, s, 2H, NH_2), 7.05 (d, J = 8.4 Hz, 1H), 2.77 (s, 6H, $N(CH_3)_2$), 2.28 (s, 3H, ArCH_3); IR (KBr): 2207 (C≡N), 1682 (C═O), 1605 (C═C), 1507, 1357, 1120, 812
2g	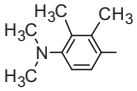	376 (13500)	35	M.p.: 194–196; ^1H NMR: 8.36 (s, 1H, –CH═), 7.88 oraz 7.70 (s, 2H, NH_2), 7.69 (d, J = 8.4 Hz, 1H), 7.00 (d, J = 8.4 Hz, 1H), 2.67 (s, 6H, $N(CH_3)_2$), 2.25 (s, 3H, ArCH_3), 2.20 (s, 3H, ArCH_3); ^{13}C NMR: 162.9 (CO), 155.7 (C), 150.1 (CH), 137.7 (C), 129.8 (C), 126.3 (CH), 124.9 (C), 116.8 (C), 115.5 (CH), 106.1 (C), 43.6 ($N(CH_3)_2$), 16.4 (ArCH_3), 15.3 (ArCH_3); IR (KBr): 2213 (C≡N), 1692 (C═O), 1567, 1377, 1266, 812
2h	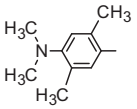	393 (17400)	75	M.p.: 214–216; ^1H NMR: 8.20 (s, 1H, –CH═), 7.84 (s, 1H), 7.80 oraz 7.63 (s, 2H, NH_2), 6.86 (s, 1H, NH_2), 2.74 (s, 6H, $N(CH_3)_2$), 2.34 (s, 3H, ArCH_3), 2.23 (s, 3H, ArCH_3); ^{13}C NMR: 163.1 (CO), 155.7 (C), 147.7 (CH), 138.6 (C), 130.7 (CH), 127.0 (C), 123.1 (C), 119.3 (CH), 117.2 (C), 103.3 (C), 42.9 ($N(CH_3)_2$) 19.3 (CH_3), 18.9 (CH_3); IR (KBr): 2216 (C≡N), 1689 (C═O), 1558, 1342, 809
2i	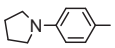	419 (45400)	49	M.p.: decomp. 215–220; ^1H NMR: 7.94 (s, 1H, –CH═), 7.84 (d, J = 8.8 Hz, 2H), 7.54 oraz 7.47 (s, 2H, NH_2), 6.65 (d, J = 9.0 Hz, 2H), 3.35 (t, 4H, NCH_2), 1.96 (t, J = 6.6 Hz, 4H, CH_2); IR (KBr): 2208 (C≡N), 1667 (C═O), 1610 (C═C), 1526, 1374, 1192, 814
2j	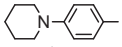	414 (36500)	69	M.p.: decomp. 195–207; ^1H NMR: 7.96 (s, 1H, –CH═), 7.83 (d, J = 8.8 Hz, 2H), 7.61 oraz 7.52 (s, 2H, NH_2), 7.02 (d, J = 9.2 Hz, 2H), 3.43 (t, J = 4.8 Hz, 4H, NCH_2), 1.59 (br, s, 6H, CH_2); IR (KBr): 2221 (C≡N), 1665 (C═O), 1605 (C═C), 1520, 1361, 1201, 808
2k	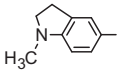	425 (37900)	73	M.p.: 190–192; ^1H NMR: 7.92 (s, 1H, –CH═), 7.77 (s, 1H), 7.62 (d, J = 8.4 Hz, 1H), 7.47 (br, s, 2H, NH_2), 6.56 (d, J = 8.4 Hz, 1H), 3.56 (t, J = 8.4 Hz, 2H, NCH_2), 3.01 (t, J = 8.0 Hz, 2H, $ArCH_2$), 2.88 (s, 3H, NCH_3); ^{13}C NMR: 163.9 (CO), 156.5 (C), 150.5 (CH), 134.6 (CH), 130.5 (C), 124.9 (CH), 119.8 (C), 118.4 (C), 105.1 (CH), 95.9 (C), 54.1 (NCH_2), 33.5 (NCH_3), 26.9 (CH_2); IR (KBr): 2201 (C≡N), 1682 (C═O), 1621 (C═C), 1517, 1364, 1295, 796
2l	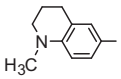	426 (29500)	61	M.p.: 167–168; ^1H NMR: 7.87 (s, 1H, –CH═), 7.67 (d, J = 8.8 Hz, 1H), 7.56 (s, 1H), 7.47 (br, s, 2H, NH_2), 6.66 (d, J = 8.8 Hz, 1H), 3.36 (t, J = 5.6 Hz, 2H, NCH_2), 2.97 (s, 3H, NCH_3) 2.68 (t, J = 5.8 Hz, 2H, $ArCH_2$), 1.86 (m, 2H, CH_2); IR (KBr): 2200 (C≡N), 1681 (C═O), 1615 (C═C), 1525, 1329, 1206, 800.
2m	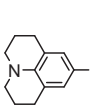	440 (33000)	78	M.p.: decomp. 180–190; ^1H NMR: 7.80 (s, 1H, –CH═), 7.42 (s, 4H, ArH and NH_2), 3.29 (t, J = 5.4 Hz, 4H, NCH_2), 2.67 (t, J = 6.2 Hz, 4H, $ArCH_2$), 1.86 (m, 4H, CH_2); ^{13}C NMR: 164.1 (CO), 150.2 (CH), 146.4 (C), 130.1 (CH), 120.2 (C), 118.6 (C), 117.5 (C), 94.9 (C), 43.2 ($N(CH_2)_2$), 27.1 (CH_2), 20.6 (CH_2); IR (KBr): 2200 (C≡N), 1684 (C═O), 1611 (C═C), 1524, 1314, 1169
2n	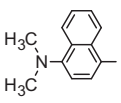	411 (16500)	44	M.p.: 201–203; ^1H NMR: 8.79 (s, 1H, –CH═), 8.21–8.12 (m, 3H), 8.08 oraz 7.76 (s, 2H, NH_2), 7.69–7.56 (m, 2H), 7.18 (d, J = 8.4 Hz, 1H), 2.95 (s, 6H, $N(CH_3)_2$); IR (KBr): 2208 (C≡N), 1702 (C═O), 1568, 1340, 1138, 763

[a] Measurements made in methanol.

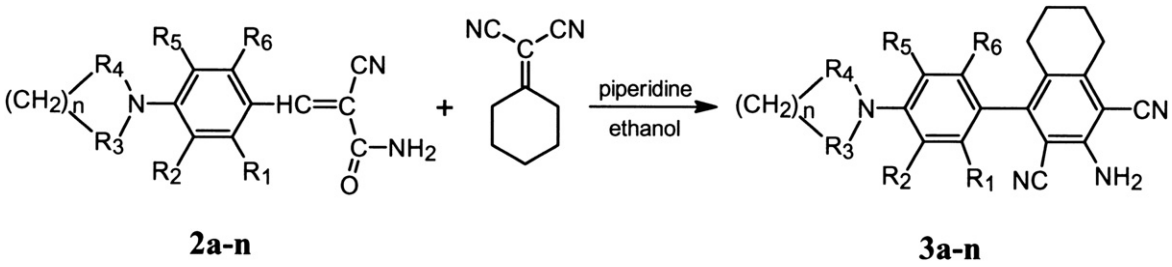

Scheme 2. A general route for the synthesis of 3,4′-diamino-2,4-dicyanobiphenyl derivatives.

route for the synthesis of the compound **3o** is presented in Scheme 3. The acylation of **3c** in refluxing acetic anhydride gives **3p**.

The structure and purity of the prepared compounds were confirmed by ^{1}H and ^{13}C NMR spectroscopy and also HPLC. The data of the structural analysis for all synthesized dyes are given in Table 2 and Supplementary data.

The yield of the reaction oscillated in the range 35–58%. Dye **3e** could not be obtained. This is probably due to too much steric hindrance, caused by two methyl groups.

3.2. Spectroscopic studies

All of the solvents used for spectroscopic studies were of the highest grade commercially available.

The electronic absorption spectra of compounds obtained in the first stage of the synthesis, 2-cyano-3-[4-aminophenyl]-2-propenamide derivatives, are shown in Fig. 1. These compounds possess the same acceptor group and various donor groups. All electronic spectra exhibit two bands whose maxima are located within a range of ca. 260 and 375–440 nm. The short wavelength bands are attributed to the $\pi \rightarrow \pi^*$ transitions, whereas the long wavelength bands, generally characterized by higher molar absorption coefficients, are attributed to an intramolecular charge transfer transition ($S_0 \rightarrow$ CT). Inspection of absorption spectra presented in Fig. 1 and data collected in Table 1 show that the position and intensity of the long-wavelength absorption band strongly depends on the structure of the amino group. Substituents in the *ortho* position with respect to the dimethylamino group (**2f**, **2g** and **2h**) form a pretwisted molecule even in the ground state. This is reflected in the electronic absorption spectra where a blue shift is observed, and absorption bands have significantly reduced intensity. It occurs, due to steric interactions, which decouple the dimethylamino group from the electron-accepting part of the molecule.

The planar conformation of the julolidine group in the **2m** dye increases the probability of radiative transitions in comparison with the other molecules (red shift).

Substituents in the *ortho* position with respect to the double bond (dyes **2e** and **2n**) have little effect on the absorption maximum but strongly reduce the molar absorption coefficient.

Similar spectral properties were observed for styrylpyridinium salts [27].

The spectroscopic properties of the tested compounds, biphenyls obtained in the second stage of the synthesis, were studied in solvents of different polarity. The characteristic properties of the long wavelength absorption and emission maxima of the studied molecules in four solvents are collected in Table 2. Fig. 2 shows the absorption spectra of selected dyes in methanol. The spectra present three main bands located in the region of 200–500 nm. The highest energy bands are located around λ_{max} = 220 nm and λ_{max} = 250 nm. The absorption maxima positions of these bands are practically independent of the solvent polarity. The maximum of the lowest energy absorption bands are located around 370 nm, and their positions depend on the solvent polarity.

As can be seen in Table 3, upon increasing the solvent polarity the long-wavelength absorption maximum is red-shifted. The shift obtained for intensely polar solvent (DMF) relative to the maximum of the lowest energy absorption band in non-polar solvent (hexane) is considerably high (usually 850–950 cm^{-1}, 1050 cm^{-1} for **3i**) suggesting quite high ground state dipole moments of these compounds.

Steady-state fluorescence spectra were recorded in the same solvents as the electronic absorption spectra. A typical example of the solvent polarity effect on the fluorescence emission spectra of molecules under the study is illustrated in Fig. 3, and summarized in Table 3.

To some extent, in low polarity solvents, the relationship between the absorption and the emission spectra displays a mirror image suggesting a weak geometrical relaxation of Franck–Condon singlet excited state. It should be underlined, however, that the Stokes' shift observed is considerably high (2280–4880 cm^{-1} in hexane) suggesting a quite substantial dipole moment change caused by the excitation.

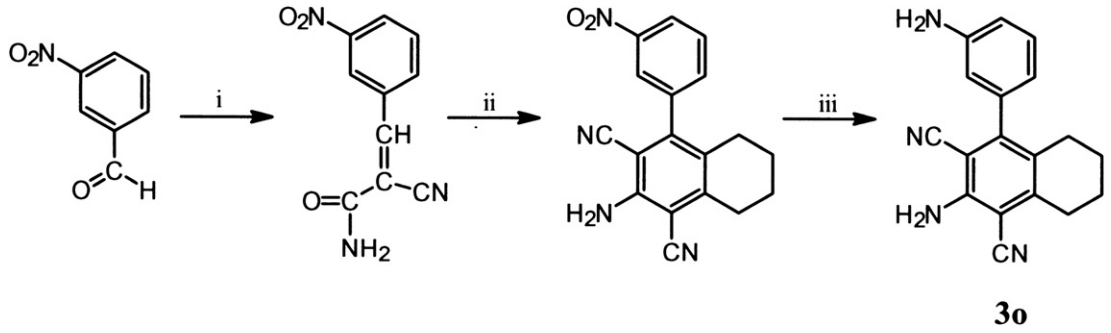

Scheme 3. A route for the synthesis of 2-amino-4-(3-aminophenyl)-5,6,7,8-tetrahydrona-phthalene-1,3-dicarbonitrile (**3o**).

Table 2
Structures, and characteristics of the tested dyes.

Ab.	Structure	Yield %	Melting point [°C], ^{1}H and ^{13}C NMR (DMSO-d_6) δ [ppm], IR (KBr) ν [cm^{-1}]
3a	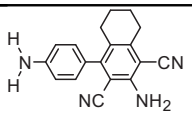	56	M.p.: 255–258; ^{1}H NMR: 6.90 (d, J = 8.4 Hz, 2H), 6.61 (d, J = 8.4 Hz, 2H), 6.28 (s, 2H, NH_2), 5.37 (s, 2H, NH_2), 2.81 (t, J = 6 Hz, 2H), 2.23 (t, J = 5.8 Hz, 2H), 1.69 (m, 2H), 1.55 (m, 2H); ^{13}C NMR: 150.9 (C), 150.6 (C), 148.9 (C), 146.1 (C), 129.1 (CH), 124.6 (C), 123.7 (C), 116.1 (C), 115.5 (C), 113.3 (CH), 95.8 (C), 94.7 (C), 29.0 (CH_2), 27.0 (CH_2), 22.1 (CH_2), 21.5 (CH_2); IR (KBr): 2211, 1643, 1521, 1272, 823, 517
3b	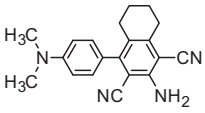	37	M.p.: 252–254; ^{1}H NMR: 7.08 (d, J = 8.8 Hz, 2H), 6.78 (d, J = 8.4 Hz, 2H), 6.29 (s, 2H, NH_2), 2.96 (s, 6H, $N(CH_3)_2$), 2.82 (t, J = 6.2 Hz, 2H), 2.23 (t, J = 6.0 Hz, 2H), 1.70 (m, 2H), 1.55 (m, 2H); ^{13}C NMR: 150.6 (C), 150.5 (C), 149.9 (C), 146.2 (C), 129.1 (CH), 124.6 (C), 124.0 (C), 116.1 (C), 115.5 (C), 111.6 (CH), 95.8 (C), 94.8 (C), 39.8 (NCH_3) 29.0 (CH_2), 27.0 (CH_2), 22.1 (CH_2), 21.5 (CH_2); IR (KBr): 2217, 1633, 1528, 1366, 810
3c	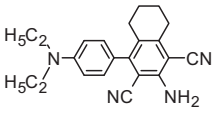	58	M.p.: 178–180; ^{1}H NMR: 7.03 (d, J = 8.8 Hz, 2H), 6.69 (d, J = 9.0 Hz, 2H), 6.26 (s, 2H, NH_2), 3.36 (q, J = 7.4 Hz, 4H, NCH_2), 2.80 (t, J = 6 Hz, 2H), 2.23 (t, J = 6 Hz, 2H), 1.69 (m, 2H), 1.54 (m, 2H), 1.10 (t, J = 6.8 Hz, 6H, CH_3); ^{13}C NMR: 150.7 (C), 150.6 (C), 147.2 (C), 146.2 (C), 129.5 (CH), 124.7 (C), 122.8 (C), 116.2 (C), 115.5 (C), 110.5 (CH), 95.7 (C), 94.7 (C), 43.5 (NCH_2), 29.0 (CH_2), 27.1 (CH_2), 22.1 (CH_2), 21.5 (CH_2), 12.5 (CH_3); IR (KBr): 2223, 1637, 1524, 1353, 813
3d	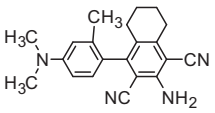	52	M.p.: 225–227; ^{1}H NMR: 6.81 (d, J = 8.2 Hz, 1H), 6.65–6.58 (m, 2H), 6.31 (s, 2H, NH_2), 2.92 (s, 6H, $N(CH_3)_2$), 2.81 (t, J = 5.9 Hz, 2H), 2.06 (m, 2H), 1.92 (s, 3H, $ArCH_3$), 1.67 (m, 2H), 1.55 (m, 2H); ^{13}C NMR: 150.7 (C), 150.6 (C), 150.2 (C), 146.5 (C), 134.8 (C) 128.4 (CH), 125.3 (C), 124.6 (C), 115.7 (C), 115.5 (C), 113.5 (CH), 110.0 (CH), 96.4 (C), 95.2 (C), 39.9 ($N(CH_3)_2$), 28.9 (CH_2), 26.4 (CH_2), 21.9 (CH_2), 21.5 (CH_2), 19.5 ($ArCH_3$); IR (KBr): 2216, 1632, 1447, 798.
3e	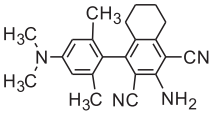	0	Compound could not be obtained
3f	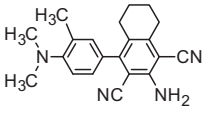	42	M.p.: 190–192; ^{1}H NMR: 7.08 (d, J = 8.8 Hz, 1H), 7.02 (s, 1H), 7.00 (d, J = 7.2 Hz, 1H), 6.35 (s, 2H, NH_2), 2.81 (t, J = 5.8 Hz, 2H), 2.68 (s, 6H, $N(CH_3)_2$), 2.27 (s, 3H, $ArCH_3$), 2.17 (m, 2H), 1.70 (m, 2H), 1.53 (m, 2H); ^{13}C NMR: 152.3 (C), 150.6 (C), 150.1 (C), 146.4 (C), 130.9 (C), 130.7 (CH), 130.4 (C), 126.4 (CH), 124.4 (C), 117.9 (CH), 115.9 (C), 115.4 (C), 95.5 (C), 95.2 (C), 43.6 ($N(CH_3)_2$) 29.0 (CH_2), 27.0 (CH_2), 22.0 (CH_2), 21.5 (CH_2), 18.4 ($ArCH_3$); IR (KBr): 2212, 1630, 1451, 1114, 820
3g	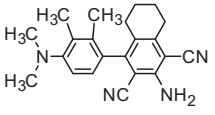	56	M.p.: 223–226; ^{1}H NMR: 6.99 (d, J = 8.2 Hz, 1H), 6.81 (d, J = 8.0 Hz, 1H), 6.40 (s, 2H, NH_2), 2.82 (t, J = 5.8 Hz, 2H), 2.22 (s, 3H, $ArCH_3$), 1.97 (m, 2H) 1.87 (s, 3H, $ArCH_3$), 1.68 (m, 2H), 1.54 (m, 2H); ^{13}C NMR: 152.3 (C), 150.7 (C), 150.5 (C), 146.5 (C), 134.0 (C), 131.1 (C), 130.4 (C), 125.3 (CH), 124.7 (C), 115.9 (CH), 115.5 (C), 115.4 (C), 95.8 (C), 95.3 (C), 44.1 ($N(CH_3)_2$) 28.9 (CH_2), 26.3 (CH_2), 21.8 (CH_2), 21.5 (CH_2), 16.7 ($ArCH_3$), 14.6 ($ArCH_3$); IR (KBr): 2222, 1644, 1452, 1282, 1042, 820
3h	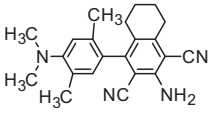	41	M.p.: 204–206; ^{1}H NMR: 6.95 (s, 1H), 6.79 (s, 1H), 6.40 (s, 2H, NH_2), 2.83 (t, J = 5.6 Hz, 2H), 2.67 (s, 6H, $N(CH_3)_2$), 2.23 (s, 3H, $ArCH_3$), 2.06 (m, 2H), 1.93 (s, 3H, $ArCH_3$), 1.69 (m, 2H), 1.57 (m, 2H); ^{13}C NMR: 152.1, 150.6, 150.0, 146.6, 132.2, 130.3, 130.1, 128.5, 124.6, 119.6, 115.5, 115.4, 95.7 (C), 95.3 (C), 43.6 ($N(CH_3)_2$), 28.9 (CH_2), 26.4 (CH_2), 21.9 (CH_2), 21.5 (CH_2), 18.8 ($ArCH_3$), 17.9 ($ArCH_3$); IR (KBr): 2219, 1636, 1567, 1448, 1276, 888
3i	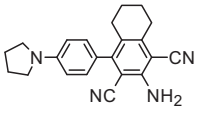	35	M.p.: 278–280; ^{1}H NMR: 7.05 (d, J = 8.6 Hz, 2H), 6.59 (d, J = 8.6 Hz, 2H), 6.26 (s, 2H, NH_2), 3.27 (t, J = 6.2 Hz, 4H, $N(CH_2)_2$), 2.81 (t, J = 6.4 Hz, 2H), 2.23 (t, J = 5.8 Hz, 2H), 1.97 (t, J = 6.4 Hz, 4H), 1.70 (m, 2H), 1.55 (m, 2H); ^{13}C NMR: 150.8 (C), 150.6 (C), 147.3 (C), 146.1 (C), 129.2 (CH), 124.7 (C), 123.0 (C), 116.1 (C), 115.5 (C), 111.1 (CH), 95.8 (C), 94.7 (C), 47.1 ($N(CH_2)_2$), 29.0 (CH_2), 27.0 (CH_2), 25.0 (CH_2), 22.1 (CH_2), 21.5 (CH_2); IR (KBr): 2217, 1632, 1525, 1376, 810
3j	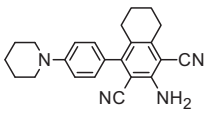	55	M.p.: 254–256; ^{1}H NMR: 7.09 (d, J = 8.8 Hz, 2H), 6.99 (d, J = 9.2 Hz, 2H), 6.33 (s, 2H, NH_2), 3.22 (t, J = 5.0 Hz, 4H, $N(CH_2)_2$), 2.82 (t, J = 6.2 Hz, 2H), 2.21 (t, J = 5.4 Hz, 2H), 1.71–1.58 (m, 10H); ^{13}C NMR: 151.0 (C), 150.6 (C), 150.3 (C), 146.3 (C), 129.1 (CH), 126.0 (C), 124.6 (C), 116.0 (C), 115.5 (C), 114.7 (CH), 95.7 (C), 95.0 (C), 48.7 ($N(CH_2)_2$), 29.0 (CH_2), 27.0 (CH_2), 25.2 (CH_2), 23.9 (CH_2), 22.1 (CH_2), 21.4 (CH_2); IR (KBr): 2217, 1631, 1518, 1238, 814
3k	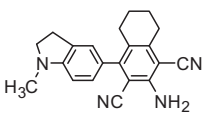	52	M.p.: 236–238; ^{1}H NMR: 6.91 (s, 1H), 6.89 (d, J = 8.8 Hz, 1H), 6.56 (d, J = 8.2 Hz, 1H), 6.29 (s, 2H, NH_2), 3.32 (t, J = 8.2 Hz, 2H, NCH_2), 2.96–2.78 (m, 4H), 2.76 (s, 3H, NCH_3), 2.22 (m, 2H), 1.70 (m, 2H), 1.54 (m, 2H); ^{13}C NMR: 153.2, 150.9, 150.6, 146.1, 129.8, 127.7, 125.5, 124.7, 124.0, 116.1, 115.5, 106.2, 95.8, 94.8, 55.2 (NCH_2), 35.3 (NCH_3), 29.0 (CH_2), 27.9 (CH_2), 27.0 (CH_2), 22.1 (CH_2), 21.5 (CH_2); IR (KBr): 2218, 1633, 1563, 1274, 809
3l	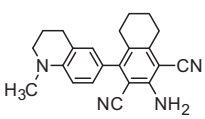	38	M.p.: 257–260; ^{1}H NMR: 6.88 (d, J = 8.4 Hz, 1H), 6.79 (s, 1H), 6.61 (d, J = 8.4 Hz, 1H), 6.27 (s, 2H, NH_2), 3.25 (t, J = 5.4 Hz, 2H, NCH_2), 2.88 (s, 3H, NCH_3), 2.81 (t, J = 6.0 Hz, 2H), 2.71 (t, J = 6.2 Hz, 2H), 2.23 (m, 2H), 1.90 (m, 2H), 1.70 (m, 2H), 1.55 (m, 2H); ^{13}C NMR: 150.6 (C), 150.6 (C) 146.3 (C), 146.1 (C), 128.3 (CH), 127.1 (CH), 124.7 (C), 123.7 (C), 121.6 (C), 116.2 (C), 115.3 (C), 110.1 (CH), 95.7 (C),

(*continued on next page*)

Table 2 (*continued*)

Ab.	Structure	Yield %	Melting point [°C], ^{1}H and ^{13}C NMR (DMSO-d_6) δ [ppm], IR (KBr) ν [cm^{-1}]
			94.7 (C), 50.4 (NCH_2), 38.5 (NCH_3), 29.0 (CH_2), 27.1 (CH_2), 27.1 (CH_2), 22.1 (CH_2), 21.6 (CH_2), 21.5 (CH_2); IR (KBr): 2216, 1631, 1520, 1228, 808
3m	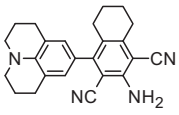	37	M.p.: decomp 228; ^{1}H NMR: 6.59 (s, 2H, ArH), 6.24 (s, 2H, NH_2), 3.16 (t, J = 5.4 Hz, 4H, $N(CH_2)_2$), 2.80 (t, J = 6.2 Hz, 2H), 2.68 (t, J = 6.4 Hz, 4H), 2.24 (t, J = 5.8 Hz, 2H), 1.88 (t, J = 5.6 Hz, 4H), 1.69 (m, 2H), 1.54 (m, 2H); ^{13}C NMR: 150.8, 150.6, 146.0, 142.5, 126.6, 124.6, 123.2, 120.2, 116.2, 115.6, 95.6, 94.5, 49.1 ($N(CH_2)_2$), 29.0 (CH_2), 27.0 (CH_2), 22.1 (CH_2), 21.5 (CH_2), 21.3 (CH_2); IR (KBr): 2207, 1629, 1562, 1311
3n	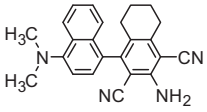	58	M.p.: 200–203; ^{1}H NMR: 8.23 (d, J = 8.4 Hz, 1H), 7.59–7.42 (m, 2H), 7.28–7.16 (m, 3H), 6.48 (s, 2H, NH_2), 2.89 (s, 6H, $N(CH_3)_2$), 2.85 (t, J = 8.0 Hz, 2H), 2.12–1.98 (m, 2H), 1.70 (m, 2H), 1.49 (m, 2H); ^{13}C NMR: 150.9 (C), 150.7 (C), 148.8 (C), 131.4 (C), 128.9 (C), 127.8 (C), 126.7 (CH), 126.3 (CH), 125.5 (C), 125.3 (CH), 124.7 (CH), 124.5 (CH), 115.6 (C), 115.4 (C), 113.4 (CH), 96.5 (C), 95.9 (C), 44.8 ($N(CH_3)_2$), 29.0 (CH_2), 26.2 (CH_2), 21.8 (CH_2), 21.5 (CH_2); IR (KBr): 2218, 1658, 1565, 1281, 1041, 767
3o	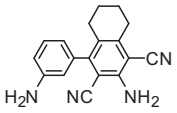		M.p.: 261–263; ^{1}H NMR: 7.11 (t, J = 7.8 Hz, 1H), 6.60 (d, J = 8.0 Hz, 1H), 6.36–6.39 (m, 4H), 5.25 (s, 2H, NH_2), 2.82 (t, J = 5.8 Hz, 2H), 2.18 (t, J = 6.4 Hz, 2H), 1.71–1.68 (m, 2H), 1.57–1.55 (m, 2H); ^{13}C NMR: 150.9 (C), 150.5 (C), 148.6 (C), 146.4 (C), 137.8 (C), 129.1 (CH), 124.0 (C), 115.7 (C), 115.4 (C), 115.0 (CH), 113.8 (CH), 113.0 (CH), 95.2 (C), 95.2 (C), 29.0 (CH_2), 26.7 (CH_2), 22.0 (CH_2), 21.5 (CH_2); IR (KBr): 2208, 1652, 1559, 1456, 1281, 792, 690
3p	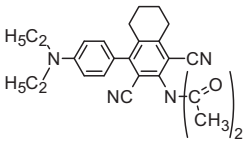		M.p.: 143–145; ^{1}H NMR: 7.18 (d, J = 8.4 Hz, 2H), 6.74 (d, J = 8.8 Hz, 2H), 3.38 (q, J = 6.6 Hz, 4H, NCH_2), 3.02 (t, J = 6.0 Hz, 2H), 2.54 (t, J = 6.0 Hz, 2H), 2.34 (s, 6H, $C(O)CH_3$), 1.80–1.77 (m, 2H), 1.66–1.64 (m, 2H), 1.11 (t, J = 7.0 Hz, 6H, CH_3); ^{13}C NMR: 171.2 (CO), 150.7, (C), 147.8 (C), 147.3 (C), 142.0 (C), 139.6 (C), 130.0 (CH), 120.9 (C), 114.5 (C), 113.8 (C), 112.6 (C), 111.8 (C), 110.6 (CH), 43.6 (NCH_2), 29.0 (CH_2), 28.3 (CH_2), 26.0 (CH_3, Ac), 21.5 (CH_2), 20.9 (CH_2), 12.5 (CH_3); IR (KBr): 2227, 1728, 1610, 1525, 1368, 1216, 820

Fig. 3 shows a typical example of the solvent effect on the electronic emission spectrum of molecules under investigation. When the solvent polarity is increased, the fluorescence band shifts to longer wavelengths. The change of the solvent polarity from low to high causes a shift of the fluorescence band of about 5000 cm^{-1}. The red shift is accompanied by a broadening of the width of the fluorescence band. As can be seen in Fig. 3, the emission spectra of a typical molecule under the study have a maximum at 398 nm, 434 nm, 476 nm and 517 nm for hexane, toluene, THF and DMF, respectively. It is observed (Table 3) that the shifts of emission peaks with increasing solvent polarity are more pronounced than the shifts of absorption peaks, which indicate that the dipole moments of the molecules increase upon excitation. The large red shifts of the emission bands indicate greater stabilization of the excited singlet state in polar solvents.

This trend is characteristic for molecules that are likely to have enlarged dipole moments and CT characters in their excited singlet states.

3.3. Electrochemical properties

The oxidation potentials of the tested compounds were determined from the cyclovoltametric measurements. The typical cyclic voltamperograms for examined biphenyls in acetonitrile are

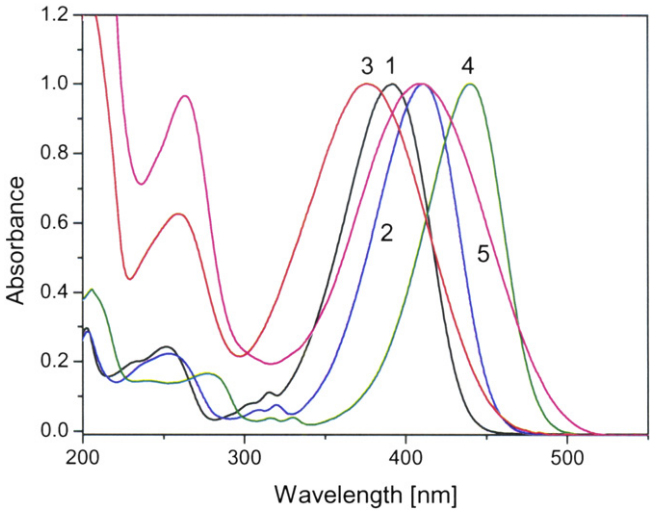

Fig. 1. Illustrative normalized electronic absorption spectra of 2-cyano-3-[4-aminophenyl]-2-propenamide derivatives in methanol: 1 – **2a**; 2 – **2b**; 3 – **2g**; 4 – **2m**; 5 – **2n**.

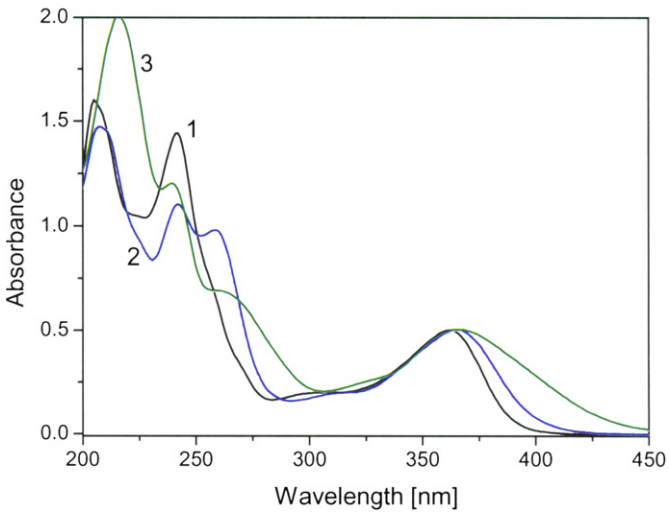

Fig. 2. Illustrative normalized electronic absorption spectra of tested dyes in methanol: 1 – **3a**; 2 – **3b**; 3 – **3m**.

Table 3
Absorption maxima wavelength (λ^{abs}_{max} [nm]), molar absorption coefficient (ε_{max} [$dm^3\ mol^{-1}\ cm^{-1}$]), fluorescence maxima wavelength (λ^{fl}_{max} [nm]), fluorescence quantum yields (Φ), Stokes' shift ($\bar{\nu}$ [cm^{-1}]) and dipole moments of the ground state (μ_g [D]).

Ab.	Hexane			Toluene				THF					DMF				μ_g
	λ^{abs}_{max}	λ^{fl}_{max}	$\bar{\nu}$	λ^{abs}_{max}	ε_{max}	λ^{fl}_{max}	$\bar{\nu}$	λ^{abs}_{max}	ε_{max}	λ^{fl}_{max}	Φ	$\bar{\nu}$	λ^{abs}_{max}	ε_{max}	λ^{fl}_{max}	$\bar{\nu}$	
3a	–	–	–	358	12,800	401	2995	365	13,500	461	0.26	5705	367	13,800	503	7367	4.76
3b	357	395	2695	364	11,700	434	4431	367	15,300	477	0.31	6284	370	16,200	519	7759	6.09
3c	365	398	2272	372	16,500	434	3840	370	16,600	476	0.52	6019	374	14,400	517	7396	6.38
3d	351	395	3174	355	9800	448	5848	361	12,000	499	0.10	7661	362	11,200	559	9735	5.43
3f	352	400	3409	357	12,000	441	5335	361	14,100	489	0.58	7251	363	12,200	533	8786	5.10
3g	350	397	3383	354	13,000	456	6319	359	10,700	501	0.28	7895	362	9900	560	9767	4.26
3h	350	399	3509	354	9730	459	6462	358	11,500	504	0.25	8092	362	10,800	566	9956	4.30
3i	359	399	2792	371	15,000	439	4175	369	17,400	479	0.46	6223	373	15,700	532	8013	6.45
3j	354	400	3249	361	12,600	438	4870	364	14,900	486	0.42	6896	367	13,800	522	8091	6.33
3k	355	412	3897	361	11,500	474	6604	366	14,700	513	0.29	7829	368	14,000	574	9752	5.62
3l	358	405	3242	365	12,500	452	5273	367	14,600	500	0.41	7248	372	15,400	542	8432	6.16
3m	369	440	4373	378	12,000	465	4950	366	12,500	506	0.25	7560	372	14,700	558	8961	5.89
3n	352	425	4880	356	16,600	474	6993	360	22,900	505	0.16	7976	363	19,300	559	9659	4.87
3o	–	–	–	355	9140	420	4359	359	10,900	496	0.06	7694	362	13,300	540	9106	3.91
3p	379	408	1875	388	10,600	464	4221	384	10,800	512	0.27	6510	390	11,700	540	7123	9.55

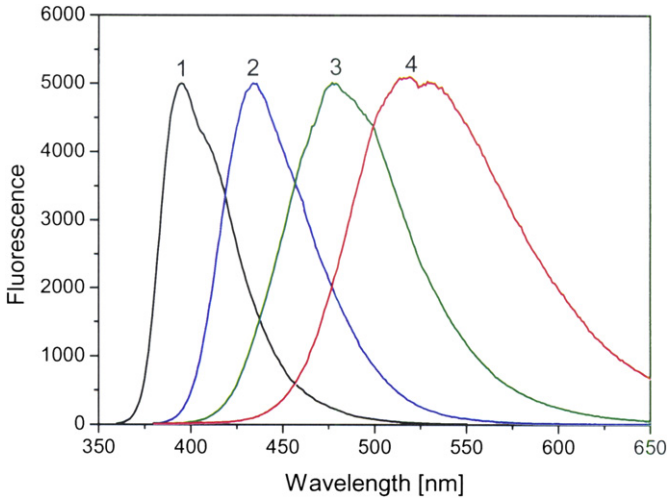

Fig. 3. Effect of the solvent polarity on normalized fluorescence spectra of **3c**. Solvent: 1 – hexane; 2 – toluene; 3 – THF; 4 – DMF.

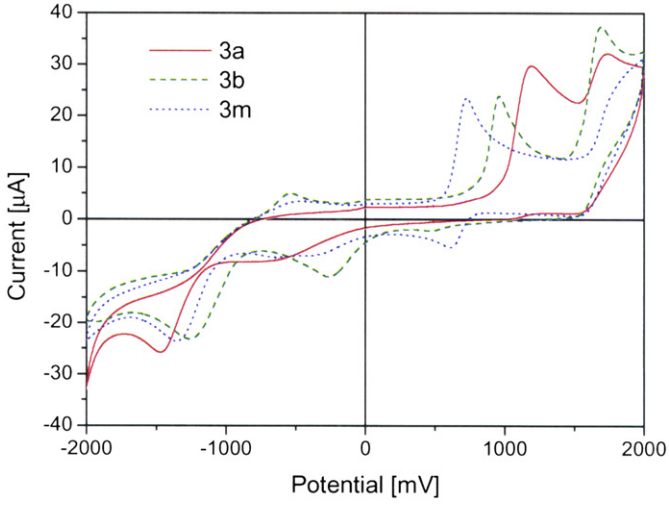

Fig. 4. Cyclic voltamperograms for selected dyes under the study in acetonitrile. Solution contained tetra-*n*-butylammonium perchlorate as the supporting electrolyte and was deoxygenated prior to analysis by purging with argon for 15 min.

Table 4
The measured oxidation potentials of the dyes under the study.

Ab.	E_{ox} [mV]	Ab.	E_{ox} [mV]	Ab.	E_{ox} [mV]
3a	1196	**3g**	1016	**3l**	842
3b	962	**3h**	972	**3m**	728
3c	956	**3i**	916	**3n**	932
3d	938	**3j**	964	**3o**	1186
3f	1036	**3k**	780	**3p**	1028

presented in Fig. 4. Analysis of the curves indicates that the electrochemical oxidation of the compounds under the study is reversible. The measured oxidation potentials of the tested biphenyls are summarized in Table 4. The difference in the oxidation potentials is indicative of the relative ease of electron removal from amino group. The structure of the amino group has therefore a major impact on oxidation potential. The compounds of higher oxidation potential, exhibit weaker electron donor properties (**3a**, **3o**).

4. Conclusions

In the two-stage synthesis reaction we have successfully synthesized a series of 15 new dyes – biphenyl derivatives possessing strong electron acceptors substituents in one phenyl ring and strong electron donor group in the *para* or *meta* position in the second ring. Their electronic absorption and steady-state fluorescence spectra have been investigated. The spectroscopic behavior of the tested dyes in solvents of different polarity has been compared. It was observed that the shifts of emission peaks with change in solvent polarity are more pronounced than the shifts of absorption peaks, indicating that the dipole moments of the molecules increase on excitation. The dyes are characterized by high fluorescence quantum yield, which was determined by the comparative method using Coumarin I as a standard.

They undergo two quasi-reversible one-electron oxidations and two quasi-reversible one-electron reductions in acetonitrile at modest potentials.

Acknowledgment

This work was supported by The Ministry of Science and Higher Education of Poland (MNiSW) (grant N N204 054335).

Appendix A. Supplementary data

Supplementary data related to this article can be found online at http://dx.doi.org/10.1016/j.dyepig.2012.07.009.

References

[1] Reichardt C. Solvents and solvent effects in organic chemistry. 2nd ed. Weinheim: VCH Verlagsgesellschaft mbH; 1988.
[2] Suppan P. Solvatochromic shifts – the influence of the medium on the energy of electronic states. J Photochem Photobiol A 1990;50:293–330.
[3] Bosch P, Catalina F, Corrales T, Peindado C. Fluorescent probes for sensing processes in polymers. Chem Eur J 2005;11:4314–25.
[4] Bajorek A, Wrześniewska I, Pietrzak M. Stilbazolium salts as fluorescence probes for monitoring local viscosity and pH of solutions. Chemik 2011;65: 255–60.
[5] Bajorek A, Pączkowski J. Influence of the attachment of chromophores to a polymer chain on their twisted intramolecular charge-transfer state in diluted solution. Macromolecules 1998;31:86–95.
[6] Jędrzejewska B, Pietrzak M, Pączkowski J. Solvent effects on the spectroscopic properties of styrylquinolinium dyes series. J Fluoresc 2010;20:73–86.
[7] Morawetz H. Fluorescence studies of polymer dynamics. J Lumin 1989;43: 59–71.
[8] Rettig W, Lapouyade R. In: Lakowicz JR, editor. Topics in fluorescence spectroscopy, probe design and chemical sensing. New York: Plenum Press; 1994. p. 109.
[9] Wang M, Holmes-Davis R, Rafinski Z, Jedrzejewska B, Choi KY, Zwick M, et al. Accelerated photobleaching of a cyanine dye in the presence of a ternary target DNA, PNA probe, dye catalytic complex: a molecular diagnostic. Anal Chem 2009;81:2043–52.
[10] Kaloyanova S, Crnolatac I, Lesev N, Piantanida I, Deligeorgiev T. Synthesis and study of nucleic acids interactions of novel monomethine cyanine dyes. Dye Pigment 2012;92:1184–91.
[11] Demchenko AP, Sytnik AI. Site selectivity in excited-state reactions in solutions. J Phys Chem 1991;95:10518–24.
[12] Demchenko AP. The red-edge effects: 30 years of exploration. Luminescence 2002;17:19–42. and references therein.
[13] Chattopadhyay A, Mukherjee S. Red edge excitation shift of a deeply embedded membrane probe: implications in water penetration in the bilayer. J Phys Chem B 1999;103:8180–5.
[14] Józefowicz M, Aleksiejew M, Heldt JR, Bajorek A, Pączkowski J, Heldt J. Spectroscopic properties of ethyl 5-(4-aminophenyl)-3-amino-2,4-dicyanobenzoate. Chem Phys 2007;338:53–61.
[15] Józefowicz M, Heldt JR, Bajorek A, Pączkowski J. Spectroscopic properties of ethyl 5-(4-dimethyl-aminophenyl)-3-amino-2,4-dicyanobenzoate. Chem Phys 2009;363:88–99.
[16] Gewald K, Schill W. Addition of alkylidenemalononitriles to activated C–C double-bonds. J Prakt Chem 1971;313:678–85.
[17] Milart P, Sepioł J. New synthesis of substituted biphenyls, biaryls, and terphenyls from arylidenemalonodinitriles, ethyl pyruvate, and malonodinitrile. Tetrahedron Lett 1990;31:2735–8.
[18] Milart P, Wilamowski J, Sepioł J. Synthesis of di- and triamino-1,1′:3′,1″-terphenyls from arylerhylidene- and arylidenemalonodinitriles. Tetrahedron 1998;54:15643–56.
[19] Raghukumar V, Murugan P, Ramakrishnan VT. A facile one pot synthesis of *m*-terphenyl and biaryl derivatives. Synth Commun 2001;31:3497–505.
[20] Elgemeie GLH, Elzanate AM, Mansour AK. Novel synthesis of indanes, tetralones, condensed benzocarbocyclic nitriles and condensed pyridine-2(1H)-thiones from the reactions of cycloalkylidene-malonitriles with arylmethylene(cyano)-acetamide and -thioacetamide. J Chem Soc Perkin Trans 1992;1:1073–4.
[21] Olmsted III J. Calorimetric determinations of absolute fluorescence quantum yields. J Phys Chem 1979;83:2571–84.
[22] Frisch MJ, Trucks GW, Schlegel HB, Scuseria GE, Robb MA, Cheeseman JR, et al. Gaussian 03, revision B.03. Pittsburgh PA: Gaussian, Inc.; 2003.
[23] Pietrzak M. To be published.
[24] Gawinecki R, Andrzejak S, Puchała A. Efficiency of the Vilsmeier-Haack method in the synthesis of *p*-aminobenzaldehydes. Org Prep Proc Int 1998; 30:455–60.
[25] Bajorek A, Trzebiatowska K, Jędrzejewska B, Pietrzak M, Gawinecki R, Pączkowski J. Developing of fluorescence probes based on stilbazolium salts for monitoring free radical polymerization processes. II. J Fluoresc 2004;14:295–307.
[26] Zabicky J. The kinetics and mechanism of carbonyl-methylene condensation reactions. Part XI. Stereochemistry of the products. J Chem Soc 1961:683–7.
[27] Gawinecki R, Trzebiatowska K. The effect of the amino group on the spectral properties of substituted styrylpyridinium salts. Dyes Pigments 2000;45: 103–7.